Two-Dimensional Nanomaterials

Deutsche Ausgabe: DOI: 10.1002/ange.201605515
Internationale Ausgabe: DOI: 10.1002/anie.201605515

Controlled Gas Exfoliation of Boron Nitride into Few-Layered Nanosheets

Wenshuai Zhu, Xiang Gao, Qian Li, Hongping Li, Yanhong Chao, Meijun Li, Shannon M. Mahurin, Huaming Li, Huiyuan Zhu,* and Sheng Dai**

Abstract: *The controlled exfoliation of hexagonal boron nitride (h-BN) into single- or few-layered nanosheets remains a grand challenge and becomes the bottleneck to essential studies and applications of h-BN. Here, we present an efficient strategy for the scalable synthesis of few-layered h-BN nanosheets (BNNS) using a novel gas exfoliation of bulk h-BN in liquid N_2 (L-N_2). The essence of this strategy lies in the combination of a high temperature triggered expansion of bulk h-BN and the cryogenic L-N_2 gasification to exfoliate the h-BN. The produced BNNS after ten cycles (BNNS-10) consisted primarily of fewer than five atomic layers with a high mass yield of 16–20 %. N_2 sorption and desorption isotherms show that the BNNS-10 exhibited a much higher specific surface area of 278 $m^2 g^{-1}$ than that of bulk BN (10 $m^2 g^{-1}$). Through the investigation of the exfoliated intermediates combined with a theoretical calculation, we found that the huge temperature variation initiates the expansion and curling of the bulk h-BN. Subseqently, the L-N_2 penetrates into the interlayers of h-BN along the curling edge, followed by an immediate drastic gasification of L-N_2, further peeling off h-BN. This novel gas exfoliation of high surface area BNNS not only opens up potential opportunities for wide applications, but also can be extended to produce other layered materials in high yields.*

Two-dimensional (2D) nanomaterials such as graphene, hexagonal boron nitride (h-BN), carbon nitride and transition metal dichalcogenides have received extensive attention due to their intriguing mechanical, electronic and thermal properties.[1] Exfoliation from layered parent materials is a widely used strategy to synthesize single- or few-layered ultrathin planar materials.[2] In 2004, graphene as a vital single-layer 2D material, was first exfoliated from graphite by a mechanical cleavage method.[3] Since then, continous interest has been given to prepare various ultrathin 2D materials.[4] As an analogue of graphite, the few-layered h-BN derived from its bulk crystal, has also been intensively studied in recent years because of its wide applications in electronics, energy storage devices and as a catalyst, an environmental adsorbent or a solid lubricant.[5] To date, few-layered h-BN nanosheets (BNNS) are mostly prepared via either a solid-phase mechanical method or liquid-phase exfoliation.[4] The solid-phase mechanical exfoliation is usually high energy/time-consuming. Although liquid exfoliation is considered to be more efficient than mechanical exfoliation,[6] it often suffers from the use of a large amount of chemical reagents, long agitation time and low yield.[7] Moreover, chemical impurities are inevitably introduced into the final few-layered h-BN and the products need additional complicated post-treatments for purification purpose. An ideal strategy for preparing few-layered h-BN should incorporate a short reaction period, nontoxic components, scalability and without the use of chemical additives.[8]

Here, we strive for an efficient synthesis of ultrathin BNNS. We first ramp the commercial h-BN (parent bulk h-BN) to 800 °C in air and immediately immerse it into the liquid N_2 (L-N_2) until the L-N_2 gasifies completely. The essence of this strategy lies in the combination of a high temperature triggered expansion of bulk h-BN and a subsequent L-N_2 gasification that exfoliates the h-BN. The reason that we choose the exfoliation of the h-BN as an example to demonstrate the interplay between thermal expansion and gas exfoliation is that h-BN is even more challenging to be exfoliated than other layered materials due to the partial ionic character in the B–N bond and the "lip-lip" interactions between neighboring layers.[9] In addition, it is appropriate to adopt the high temperature treatment without destroying the h-BN structure or introducing any impurities because of the high thermostability of h-BN in air and N_2 (see the Supporting Information Figure S1). As shown in Scheme 1, when h-BN is heated to high temperature (800 °C), the interlayer distance and volume should expand.[10] As a result, the van der Waals force between interlayers and the lip-lip interactions of h-BN weaken at such a high temperature. Then, the h-BN is immediately dipped into the cryogenic L-N_2 (−196 °C). The instant local temperature variation (800 °C vs. −196 °C) not

[*] Dr. W. S. Zhu, Dr. H. P. Li, Dr. Y. H. Chao, Prof. H. M. Li
School of Chemistry and Chemical Engineering
Institute for Energy Research, Jiangsu University
Zhenjiang 212013 (China)
E-mail: zhuws@ujs.edu.cn
Dr. W. S. Zhu, Dr. S. M. Mahurin, Dr. H. Y. Zhu, Prof. S. Dai
Chemical Science Division, Oak Ridge National Laboratory
Oak Ridge, TN 37831 (USA)
E-mail: zhuh@ornl.gov
dais@ornl.gov
Dr. X. Gao
Materials Science and Technology Division, Oak Ridge National Laboratory
Oak Ridge, TN 37831 (USA)
Dr. Q. Li
Center for nanophase materials sciences, Oak Ridge National Laboratory
Oak Ridge, TN 37831 (USA)
Dr. M. J. Li, Prof. S. Dai
Department of Chemistry, University of Tennessee
Knoxville, TN 37996 (USA)

Supporting information for this article can be found under: http://dx.doi.org/10.1002/anie.201605515.

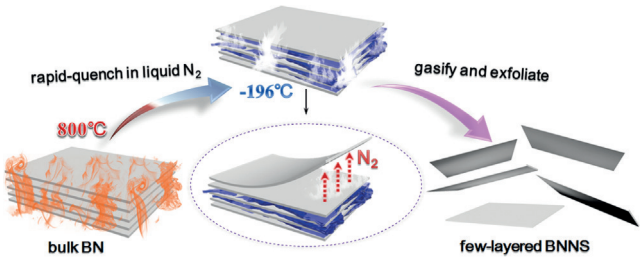

Scheme 1. Gas exfoliation of h-BN triggered by thermal expansion.

only leads to the curling and delamination of the h-BN, but also triggers the drastic expansion of L-N_2 into gaseous N_2 and exfoliates h-BN. N_2 molecules can enter from the curling edge of the h-BN and gradually penetrate into the interlayers along the fissure. The above steps are repeated for several cycles to achieve a complete exfoliation. Here BNNS-10 denotes the few-layered BNNS prepared after ten repeated cycles. The products containing ultrathin BNNS were finally collected without post-treatment. The yield of ultrathin BNNS-10 (mostly 1–5 layers) is about 16–20% by weight. This process is environmentally friendly since thermal energy is readily available and L-N_2 is a nontoxic medium that can be evaporated away after reaction, leaving no impurities in the product.

In order to illustrate the morphology change after the gas exfoliation, scanning electron microscopy (SEM) images of the parent bulk h-BN and BNNS-10 are shown in Figure 1a and Figure S2a. Compared with the bulky h-BN precursors, the BNNS-10 demonstrate a much smaller size and a nanosheet-like morphology. Meanwhile, transmission electron microscopy (TEM) images of BNNS-10 and the bulk BN also exhibit distinct differences. Figure 1b shows that the BNNS-10 has an ultrathin, transparent and overlapped flat structure, whereas a bulky and opaque structure is observed for the parent h-BN (see Figure S2b), which provides clear evidences that the h-BN sheets are exfoliated thoroughly into very thin layers. To further probe the thickness and the structural information of the as-made BNNS-10, atomic force microscopy (AFM), high-resolution annular dark-field (ADF) imaging and scanning transmission electron microscopy (STEM) were performed. As shown in the line-scan profile of BNNS-10 [16–20% yield; Figure 1c(A–C)], the thickness of the most BNNS-10 is less than 3 nm. Given that the thickness of a single-layered h-BN is about 0.4–0.5 nm,[11,12] this observation suggests that the as-prepared BNNS-10 consist mostly of 1–5 atomic layers. The AFM of BNNS-10 (Figure S3) including a three dimenstional (3D) demonstration of a thin piece (Figure 1d) show that the lateral sizes of BNNS-10 are in the range of 50–500 nm, indicating that the as-prepared BNNS-10 have a reasonable aspect ratio. A STEM image is shown in Figure 1e, which exhibits a representative terraced five-atomic-layered structure. The analysis of electron energy loss spectroscopy (EELS) edge structure in Figure 1f demonstrates that B

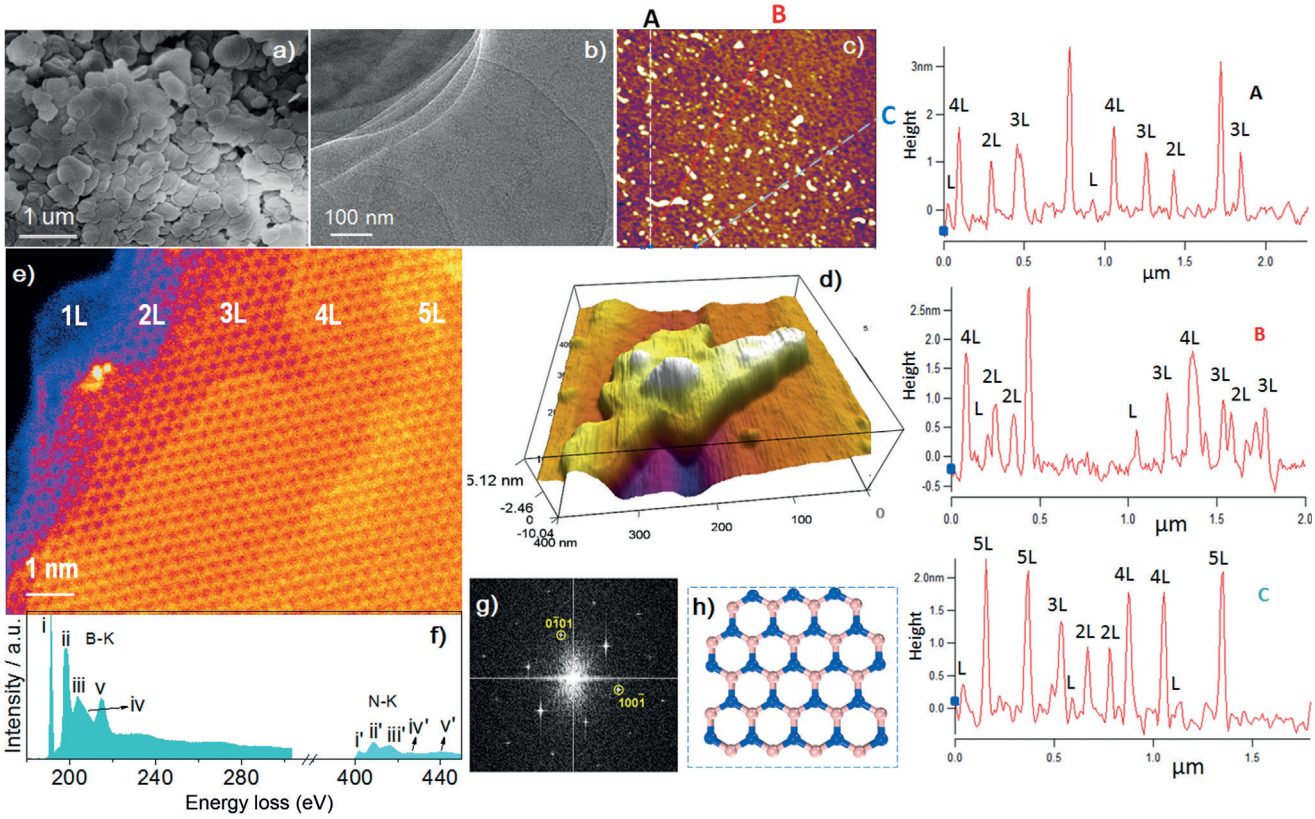

Figure 1. Characterization of exfoliated BNNS-10. a) SEM of BNNS-10; b) TEM of BNNS-10; c) AFM image and the corresponding height profiles of BNNS-10(A, B and C), L denotes layer; d) 3D demonstration of BNNS-10; e) STEM of BNNS-10; f) EELS of BNNS-10; g) The electron diffraction pattern of BNNS-10; h) hexagonal structure.

and N atoms are sp^2 hybridized in a hexagonal conformation.[11] The main peaks were labeled from i to v and i′ to v′. Peaks i, i′, ii, and ii′ are associated mainly with 1s to π* and 1s to σ* transitions, respectively. Peaks iii, iii′ originate from the antibonding interactions involving *N*-2s and B-$2p_{xy}$ orbitals. On the other hand, peaks iv and iv′ are attributed to the antibonding interactions between *N*-$2p_{xy}$ orbitals and B-$2p_{xy}$ orbitals. Peaks v and v′ can be assigned to a σ* resonance.[13] The electron diffraction pattern suggests BNNS-10 has the typical six-fold symmetry of h-BN. (Figure 1 g and 1 h).

To further characterize the crystalline structure of the exfoliated BNNS-10, X-ray powder diffraction (XRD) was carried out. Figure 2 a reveals a typical hexagonal structure of

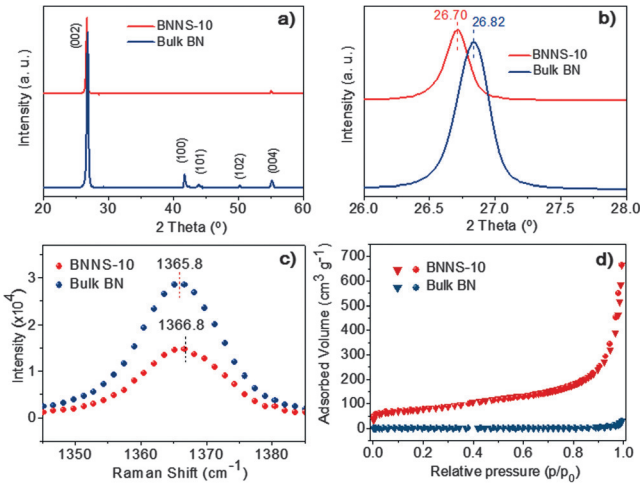

Figure 2. Structure characterizations of bulk BN and BNNS-10 a) and b) XRD; c) Raman; d) N_2-desorption and sorption isotherms.

the bulk h-BN with lattice parameters $a = b = 2.5040$ (Å) and $c = 6.6612$ (Å) of h-BN (JCPDS card no. 01-073-2095), whereas the exfoliated BNNS-10 show that the intensity of the (002) peak significantly decreases and two-theta peak slightly downshifts from 26.82 to 26.70 degree (Figure 2 b), corresponding to an increase in the interplanar distance from 3.3 Å to 3.4 Å. The increased interplanar distance and the decreased intensity of other diffraction peaks [(100), (101), (102), (004)] suggest the formation of ultrathin h-BN sheets with a less extended/ordered stacking in the *c* direction.[7a,14] These results further confirm that this gas exfoliation method can effectively flake h-BN into ultrathin layers.

We probed the Raman spectra frequency and the full widths at half-maximum (FWHM) of the G band for both bulk h-BN and BNNS-10 in order to provide detailed information on the exfoliated BNNS. The G band frequency of BNNS-10 upshifts compared with that of the bulk BN, (1366.8 cm^{-1} vs. 1365.8 cm^{-1}; Figure 2 c and Figure S4). The G band shift can be attributed to the reduction of the h-BN layers, which leads to a higher in-plane strain and weaker interlayer interaction.[12] The G band of h-BN broadens after exfoliation with an increase of the FWHM from 16.3 cm^{-1} (bulk h-BN) to 16.7 cm^{-1} (BNNS-10). This increased FWHM may be attributed to the stronger surface scattering after exfoliation, which in turn influences the vibrational excitation lifetime.[15]

Another important advantage of this novel gas exfoliation is the dramatically increased accessible surface area of BNNS-10. For catalytic or adsorptive materials, this high surface area can primarily enhance their reactivity.[16] Herein, the Brunauer–Emmett–Teller (BET) analysis of N_2 sorption and desorption isotherms show that both the bulk h-BN and BNNS-10 belong to type II isotherm based on the IUPAC classification (Figure 2 d). BNNS-10 exhibits a much higher specific surface area of 278 $m^2 g^{-1}$ than that of bulk h-BN (10 $m^2 g^{-1}$). The large increase in surface area of the BNNS-10 further suggests that this developed gas exfoliation method is highly efficient for generating single- and few-layered h-BN nanosheets.

The BNNS-10 were further analyzed by the Fourier transform infrared (FTIR), X-ray photoelectron spectroscopy (XPS) and X-ray absorption near-edge structure (XANES) for more detailed structural information. FTIR spectra in Figure S5 show the characteristic peaks of in plane B–N stretching vibrations at about 1370 cm^{-1} and B–N–B out of plane bending at about 807 cm^{-1}. The high-resolution XPS results of B 1S and N 1S are shown in Figure S6. The main peaks with a binding energy of 190.4 eV in the B 1s and 398.3 eV in the N 1s correspond to B–N bonds in BNNS-10, which are in close agreement with the reported data.[17] Figure S7 shows the B and N K-edge XANES of BNNS-10. It can be seen that the BNNS-10 exhibit features that are identical to h-BN crystals: a sharp π*(B–N) peak at 192.0 eV, a doublet σ*(B–N) resonance at 198.1 and 199.5 eV and π*(N–B), σ*(N–B) peaks at 403.2, 409.8, and 417.2 eV.[18] These observations further prove that the structure of h-BN was highly stable during the gas exfoliation process.

In order to better understand the mechanism behind this thermal-expansion-triggered gas exfoliation, we performed a series of control experiments. First, the parent bulk h-BN was ramped to 800 °C in air and naturally cooled to ambient in the absence of L-N_2. Accordingly, the SEM and TEM results for this sample summarized in Figure S8 clearly show a bulky morphology, indictating that thermal expansion alone does not exfoliate the bulk h-BN and L-N_2 plays an indispensable role in the exfoliation process. Next, the BNNS intermediate obtained via this gas exfoliation triggered by the thermal expansion with fewer repeated cycles was prepared and characterized. BNNS-3 denotes the few-layered BNNS intermediate prepared using three repeated cycles. The SEM in Figure S9 a shows that the as-prepared BNNS-3 exhibits a sheet-like structure. Meanwhile, TEM in Figure S9 b shows that some sheets in BNNS-3 exhibit transparent and overlapped flat structure, different from that of the h-BN produced by only thermal expansion treatment. These results directly indicate that the gasification of L-N_2 plays an important role during the gas exfoliation process. In order to further elucidate the role of L-N_2, we analyzed the height variation of BNNS-3 by AFM. As shown in Figure 10 and S11, the height of BNNS-3 is more than ten nanometers, much thicker than that of BNNS-10. In addition, a clear terraced morphology showing the single and few-layered BNNS near

edge joined to the multi-layered BNNS can be observed (Figure S11). Based on this phenomenon, we infer that the edge of the h-BN curled first after the enormous temperature variation.[10] Then, the gasification of L-N_2 peeled off the h-BN from the curling edge, which is also proved by the TEM and STEM of the curling BNNS intermediate (Figure S12). These results further demonstrate that the thermal expansion and L-N_2 gasification play a synergistic role to exfoliate bulk h-BN. When h-BN at high temperature is immersed in the L-N_2, the huge temperature difference between the surface and the bulk initiates the curling of h-BN edge. Subsequently, the L-N_2 penetrates into the interlayers of the bulk h-BN, where the L-N_2 gasifies and expands drastically, further exfoliating the h-BN. With controllable multiple exfoliation cycles, single- and few-layered BNNS can be successfully produced.

To further understand the mechanism of the gas exfoliation of h-BN, a model based on the above experiments was proposed. This model is an illustration of the insertion of N_2 molecules into the interlayer of two-layered h-BN, which is explored by dispersion-corrected density functional theory (DFT) at the B3LYP-D3/6-31 + G(d) level (Figure S13). The optimized distance between the interlayer of h-BN is 3.41 Å. The initial structure for N_2 insertion is a parallelled model. After N_2 insertion, the final optimized structure of h-BN layer is tilted, indicating that gas exfoliation of h-BN is possible. In addition, the exfoliation process of h-BN is endothermic because it should overcome the van der Waals force and lip-lip interaction between layers. The interaction energy was calculated to be $-10.6\,kcal\,mol^{-1}$ at 25 °C according to the current two layer model. However, the interaction energy reduced to $-6.4\,kcal\,mol^{-1}$ at 800 °C, indicating that the increase of temperature weakens the interaction between the interlayers of the h-BN. These results suggest that the thermal expansion triggers the following gas exfoliation.

In conclusion, an efficient thermal expansion triggered gas exfoliation method to prepare BNNS was successfully developed. This method has the advantages of using no chemical reagents, high yield, short reaction period, easy to be scaled up and low energy consuming. The produced BNNS demonstrate a well-defined nanosheets morphology and a high specific surface area. This novel gas exfoliation process may be extended to prepare other layered materials with optimizing reaction parameters.

Experimental Section

In a typical preparation process of BNNS, the commerciaL h-BN (parent bulk h-BN, lateral size 1 μm) powder (1 g) in quartz boat was ramped to 800 °C in muffle furnace under air, kept at this temperature for 5 minutes, and then immediately immersed into a Dewar bottle containing L-N_2 until the L-N_2 gasified completely. The above steps were performed repeatedly. The yield of BNNS-10 (mostly 1–5 atomic layers) was determined by the following process: the as-prepared BNNS-10 were dispersed in alcohol and sonicated for 30 minutes. Then the dispersion was centrifuged at 800 rpm for 10 minutes to remove any remaining bulk crystals. The supernatant was collected and dried in vacuum oven overnight. The final yield was calculated by the weight ratio between the BNNS and the parent bulk h-BN.

Acknowledgements

W.S.Z., H.Y.Z., and S.D. conceived the idea. W.S.Z. exfoliated and characterized BN. X.G. carried out STEM and EELS. Q.L. performed AFM. H.P.L., Y.H.C. and H.M.L. provided theoretical calculation and discussion. M.J.L. and S.M. performed TEM and Raman. W.S.Z. and H.Y.Z. wrote the paper. Y.H.C., H.M.L. and S.D. discussed the results and participated in the preparation of the paper. W.S.Z. and Y.H.C. appreciates the financial support from the National Natural Science Foundation of China (grant numbers 21376111, 21576122, and 21506083) and Six Big Talent Peak in Jiangsu province (JNHB-004). S.D. and S.M. were supported by the U.S. Department of Energy, Office of Science, Basic Energy Sciences, Chemical Sciences, Geosciences, and Biosciences Division. H.Z. was supported by Liane B. Russell Fellowship sponsored by the Laboratory Directed Research and Development Program at the Oak Ridge National Laboratory, managed by UT-Battelle, LLC, for the US Department of Energy. We are grateful to Dr. Chenghao Wu for his help on XANES and XPS characterizations, and Dr. Yunchao Li for his help on SEM characterization.

Keywords: boron nitride · exfoliation · liquid nitrogen · nanosheets · thermal expansion

How to cite: *Angew. Chem. Int. Ed.* **2016**, *55*, 10766–10770
Angew. Chem. **2016**, *128*, 10924–10928

[1] a) Z. Liu, Y. J. Gong, W. Zhou, L. L. Ma, J. J. Yu, J. C. Idrobo, J. Jung, A. H. MacDonald, R. Vajtai, J. Lou, P. M. Ajayan, *Nat. Commun.* **2013**, *4*, 2541; b) X. Huang, C. L. Tan, Z. Y. Yin, H. Zhang, *Adv. Mater.* **2014**, *26*, 2185–2204.

[2] a) J. N. Coleman, M. Lotya, A. O'Neill, S. D. Bergin, P. J. King, U. Khan, K. Young, A. Gaucher, S. De, R. J. Smith, I. V. Shvets, S. K. Arora, G. Stanton, H. Y. Kim, K. Lee, G. T. Kim, G. S. Duesberg, T. Hallam, J. J. Boland, J. J. Wang, J. F. Donegan, J. C. Grunlan, G. Moriarty, A. Shmeliov, R. J. Nicholls, J. M. Perkins, E. M. Grieveson, K. Theuwissen, D. W. McComb, P. D. Nellist, V. Nicolosi, *Science* **2011**, *331*, 568–571; b) V. Nicolosi, M. Chhowalla, M. G. Kanatzidis, M. S. Strano, J. N. Coleman, *Science* **2013**, *340*, 1226419; c) X. B. Fan, P. T. Xu, Y. G. C. Li, D. K. Zhou, Y. F. Sun, M. A. T. Nguyen, M. Terrones, T. E. Mallouk, *J. Am. Chem. Soc.* **2016**, *138*, 5143–5149; d) J. Kim, S. Kwon, D. H. Cho, B. Kang, H. Kwon, Y. Kim, S. O. Park, G. Y. Jung, E. Shin, W. G. Kim, H. Lee, G. H. Ryu, M. Choi, T. H. Kim, J. Oh, S. Park, S. K. Kwak, S. W. Yoon, D. Byun, Z. Lee, C. Lee, *Nat. Commun.* **2015**, *6*, 8294.

[3] K. S. Novoselov, A. K. Geim, S. V. Morozov, D. Jiang, Y. Zhang, S. V. Dubonos, I. V. Grigorieva, A. A. Firsov, *Science* **2004**, *306*, 666–669.

[4] a) A. K. Geim, *Science* **2009**, *324*, 1530–1534; b) H. Zhang, *ACS Nano* **2015**, *9*, 9451–9469; c) C. L. Tan, P. Yu, Y. L. Hu, J. Z. Chen, Y. Huang, Y. Q. Cai, Z. M. Luo, B. Li, Q. P. Lu, L. H. Wang, Z. Liu, H. Zhang, *J. Am. Chem. Soc.* **2015**, *137*, 10430–10436.

[5] a) A. Pakdel, Y. Bando, D. Golberg, *Chem. Soc. Rev.* **2014**, *43*, 934–959; b) X. F. Jiang, Q. H. Weng, X. B. Wang, X. Li, J. Zhang, D. Golberg, Y. Bando, *J. Mater. Sci. Technol.* **2015**, *31*, 589–598.

[6] a) K. G. Zhou, N. N. Mao, H. X. Wang, Y. Peng, H. L. Zhang, *Angew. Chem. Int. Ed.* **2011**, *50*, 10839–10842; *Angew. Chem.* **2011**, *123*, 11031–11034; b) G. R. Bhimanapati, D. Kozuch, J. A.

Robinson, *Nanoscale* **2014**, *6*, 11671 – 11675; c) F. Xiao, S. Naficy, G. Casillas, M. H. Khan, T. Katkus, L. Jiang, H. K. Liu, H. J. Li, Z. G. Huang, *Adv. Mater.* **2015**, *27*, 7196 – 7203; d) C. Y. Zhi, Y. Bando, C. C. Tang, H. Kuwahara, D. Golberg, *Adv. Mater.* **2009**, *21*, 2889 – 2893; e) A. Ciesielski, S. Haar, M. El Gemayel, H. F. Yang, J. Clough, G. Melinte, M. Gobbi, E. Orgiu, M. V. Nardi, G. Ligorio, V. Palermo, N. Koch, O. Ersen, C. Casiraghi, P. Samori, *Angew. Chem. Int. Ed.* **2014**, *53*, 10355 – 10361; *Angew. Chem.* **2014**, *126*, 10523 – 10529; f) X. L. Li, X. P. Hao, M. W. Zhao, Y. Z. Wu, J. X. Yang, Y. P. Tian, G. D. Qian, *Adv. Mater.* **2013**, *25*, 2200 – 2204; g) S. B. Yang, Y. J. Gong, J. S. Zhang, L. Zhan, L. L. Ma, Z. Y. Fang, R. Vajtai, X. C. Wang, P. M. Ajayan, *Adv. Mater.* **2013**, *25*, 2452 – 2456.

[7] a) P. Thangasamy, M. Sathish, *CrystEngComm* **2015**, *17*, 5895 – 5899; b) R. Bari, D. Parviz, F. Khabaz, C. D. Klaassen, S. D. Metzler, M. J. Hansen, R. Khare, M. J. Green, *Phys. Chem. Chem. Phys.* **2015**, *17*, 9383 – 9393; c) K. L. Marsh, M. Souliman, R. B. Kaner, *Chem. Commun.* **2015**, *51*, 187 – 190; d) T. Morishita, H. Okamoto, Y. Katagiri, M. Matsushita, K. Fukumori, *Chem. Commun.* **2015**, *51*, 12068 – 12071; e) Y. Lin, T. V. Williams, J. W. Connell, *J. Phys. Chem. Lett.* **2010**, *1*, 277 – 283; f) J. H. Warner, M. H. Rummeli, A. Bachmatiuk, B. Buchner, *ACS Nano* **2010**, *4*, 1299 – 1304; g) Z. Liu, Y. B. Wang, Z. Y. Wang, Y. G. Yao, J. Q. Dai, S. Das, L. B. Hu, *Chem. Commun.* **2016**, *52*, 5757 – 5760.

[8] Z. H. Cui, A. J. Oyer, A. J. Glover, H. C. Schniepp, D. H. Adamson, *Small* **2014**, *10*, 2352 – 2355.

[9] a) D. Golberg, Y. Bando, Y. Huang, T. Terao, M. Mitome, C. C. Tang, C. Y. Zhi, *ACS Nano* **2010**, *4*, 2979 – 2993; b) D. Lee, B. Lee, K. H. Park, H. J. Ryu, S. Jeon, S. H. Hong, *Nano Lett.* **2015**, *15*, 1238 – 1244.

[10] J. Zheng, H. T. Liu, B. Wu, Y. L. Guo, T. Wu, G. Yu, Y. Q. Liu, D. B. Zhu, *Adv. Mater.* **2011**, *23*, 2460 – 2463.

[11] L. Song, L. J. Ci, H. Lu, P. B. Sorokin, C. H. Jin, J. Ni, A. G. Kvashnin, D. G. Kvashnin, J. Lou, B. I. Yakobson, P. M. Ajayan, *Nano Lett.* **2010**, *10*, 3209 – 3215.

[12] L. H. Li, J. Cervenka, K. Watanabe, T. Taniguchi, Y. Chen, *ACS Nano* **2014**, *8*, 1457 – 1462.

[13] N. L. McDougall, R. J. Nicholls, J. G. Partridge, D. G. McCulloch, *Microsc. Microanal.* **2014**, *20*, 1053 – 1059.

[14] W. W. Lei, V. N. Mochalin, D. Liu, S. Qin, Y. Gogotsi, Y. Chen, *Nat. Commun.* **2015**, *6*, 8849.

[15] R. V. Gorbachev, I. Riaz, R. R. Nair, R. Jalil, L. Britnell, B. D. Belle, E. W. Hill, K. S. Novoselov, K. Watanabe, T. Taniguchi, A. K. Geim, P. Blake, *Small* **2011**, *7*, 465 – 468.

[16] a) P. W. Wu, W. S. Zhu, Y. H. Chao, J. S. Zhang, P. F. Zhang, H. Y. Zhu, C. F. Li, Z. G. Chen, H. M. Li, S. Dai, *Chem. Commun.* **2016**, *52*, 144 – 147; b) Q. H. Weng, X. B. Wang, Y. Bando, D. Golberg, *Adv. Energy Mater.* **2014**, *4*, 1301525.

[17] M. Du, X. L. Li, A. Z. Wang, Y. Z. Wu, X. P. Hao, M. W. Zhao, *Angew. Chem. Int. Ed.* **2014**, *53*, 3645 – 3649; *Angew. Chem.* **2014**, *126*, 3719 – 3723.

[18] L. J. Liu, T. K. Sham, W. Q. Han, *Phys. Chem. Chem. Phys.* **2013**, *15*, 6929 – 6934.

Received: June 6, 2016
Published online: July 22, 2016

